Engineering Structures 114 (2016) 1–13

Contents lists available at ScienceDirect

Engineering Structures

journal homepage: www.elsevier.com/locate/engstruct

Experimental study of composite beams having a precast geopolymer concrete slab and deconstructable bolted shear connectors

Abdolreza Ataei, Mark A. Bradford *, Xinpei Liu

Centre for Infrastructure Engineering and Safety, School of Civil and Environmental Engineering, UNSW Australia, Sydney, NSW 2052, Australia

ARTICLE INFO

Article history:
Received 23 August 2015
Revised 26 October 2015
Accepted 27 October 2015
Available online 15 February 2016

Keywords:
Bolted shear connectors
Geopolymer concrete slabs
Deconstructability
Composite beam
Sustainability

ABSTRACT

Traditional steel–concrete composite beams are known to exhibit excellent structural characteristics, in terms of their stiffness and strength, when compared with bare steel or reinforced concrete beams. However, within current paradigms of lowering carbon emissions and enhancing the possibly of material recycling, such traditional composite beams cannot be deconstructed easily and their elements are not recyclable because they rely on welded headed stud connectors that are encased within cast *in situ* concrete to achieve the necessary shear connection. This paper presents the detailed results of quasi-static tests conducted on full-scale composite beams as part of a novel deconstructable and sustainable structural system. For this system, precast concrete slabs are attached to a steel beam using tensioned high-strength friction-grip bolts in clearance holes as the elements to provide the shear connection. The precast slabs are made using geopolymer concrete in lieu of concrete made from ordinary Portland cement, whose manufacture is a major contributor to anthropogenic CO_2 emissions worldwide, thereby enhancing the low-carbon attributes of the structural system. The test results demonstrate the very significant ductility of the beams, with substantial interface slips being developed and sustained at loads close to the ultimate strength limit state. The tension induced in the bolts provides sufficient frictional resistance between the precast slabs and steel beams to ensure that the composite system has full shear interaction throughout the range of service loading. It is also confirmed that composite beams with bolted shear connectors can be deconstructed easily at the end of their service life, with the slabs, steel beams and bolts being reusable in other structural applications.

1. Introduction

Composite steel–concrete beams and slabs are popular components in modern steel-framed buildings, owing to their excellent structural performance in terms of stiffness and strength, their relative ease of construction and the significant economic benefits that accrue to this structural form. Such beams have higher stiffnesses and strengths, reduced deflections and higher span to depth ratios than traditional bare steel or concrete beams, by taking advantage of the favourable compressive strength of the concrete slab and the high tensile strength of the steel joist in a symbiotic configuration. The composite action between the two components is achieved almost universally by using headed stud shear connectors that are welded to the top flange of the steel beam and which are embedded in the cast *in situ* concrete slab. In response to changes of urban land use, many medium-rise buildings have relatively short structural lives and require demolition. Traditional composite beams are not conducive to deconstruction and their demolition is wasteful, energy-intensive and environmentally-intrusive, owing to the casting of the concrete around the shear studs that are welded to the top flange of the steel joist and to the reinforcement within the slab. To circumvent the shortfalls of traditional composite construction from an environmental perspective, this paper proposes the use of composite beams having precast concrete slabs that are attached to the steel joist by high-strength tensioned friction-grip bolts acting as shear connectors through clearance holes. This system is shown to be deconstructable with relative ease, and with all components being recyclable. In addition, the slabs are cast from geopolymer concrete (GPC) as a replacement for concrete using ordinary Portland cement, whose manufacture is known to be a major contributor to anthropogenic CO_2 emissions.

Research on the use of bolts as shear connectors in composite beam dates back to the late 60s. Twelve push tests on high-strength bolts as shear connectors were carried out and reported by Dallam [1]. In these series of tests, the bolts were embedded in the concrete slab and post-tensioned by the turn-of-nut method after the concrete had reached its 28-day compressive strength.

* Corresponding author. Tel.: +61 2 9385 5014; fax: +61 2 9385 9747.
E-mail address: m.bradford@unsw.edu.au (M.A. Bradford).

http://dx.doi.org/10.1016/j.engstruct.2015.10.041
0141-0296/

Dallam [1] noted that high-strength bolted connectors had a higher load capacity (about twice) of that of stud shear connectors. Subsequently, six full-scale simply supported composite beams with high-strength bolted shear connectors were tested by Dallam and Harpster [2], with the bolts being embedded in the concrete slab in the same way as for the push tests [1]. It was concluded that the high-strength bolted shear connectors provide a very rigid connection (with a high level of composite efficiency) between the steel beam and concrete slab under service loads, and that a reserve capacity sufficient for the development of the ultimate moment of the fully composite section was also attainable. Marshall et al. [3] appear to be the first investigators to report the use of bolted shear connectors through pre-drilled holes, but the context of the application is not entirely clear in their study. Three decades later, a series of individual shear connector tests was conducted on three types of post-installed shear connectors under static and fatigue loading by Kwon et al. [4]. The results showed that bolted shear connectors exhibit significantly higher fatigue strengths than those of stud shear connectors. Kwon et al. [5] also tested five full-scale beams, in order to investigate the feasibility of using bolted shear connectors for retrofitting non-composite bridge girders. It was found that the strength and stiffness of a non-composite bridge girder could be significantly improved by using post-installed bolted connectors. Recently, a number of numerical and experimental studies have been conducted on the use of high-strength friction-grip bolts as shear connectors [6–15].

The purpose of this paper is to present a comprehensive experimental study of the behaviour of composite steel–concrete beams with post-installed friction-grip bolted shear connectors (PFBSCs) and precast GPC slabs, as a replacement for traditional composite steel–concrete beams whose environmental shortcomings have been described in the above. The detailed results of quasi-static tests on four full-scale composite beams are reported, which comprise of three composite beams with PFBSCs and one with Single-nut Embedded Bolted Shear Connectors (SEBSCs) as a reference beam. The structural responses of the composite beams are assessed under a monotonically increasing static load, and the influences of the type of bolted shear connector and the degree of shear connection on the performance of the beams are evaluated. The paper also outlines the design procedure, construction and preparation of the specimens, the testing procedure, the test set-up and the instrumentation used to measure the response during the tests. The results provide benchmark studies for numerical models or for the development of design procedures.

2. Test specimens

2.1. General

The test specimens comprised of four full-scale composite beams, *viz.* three composite beams with PFBSCs and a companion beam with SEBSCs that was designed and tested as a reference for comparison. The schematic outline of the deconstructable composite beam and the cross-sectional configurations of the PFBSCs are shown in Figs. 1 and 2 respectively, and details of the specimens are summarised in Table 1. The specimens were simply supported with the total length of 7300 m with a spacing of between the supports of 7000 mm. All composite beams had a 460UB67.1 steel beam section and the reinforced square GPC slabs for the PFBSC specimens had a length of 1000 mm, an effective width of 1000 mm [16] and a thickness of 150 mm; the slab for the SEBSC specimen was 7300 mm long, had an effective width of 1000 mm [16] and was 150 mm thick.

Specimen CB1 was designed and constructed as a control specimen or reference beam, with which to compare the test results for

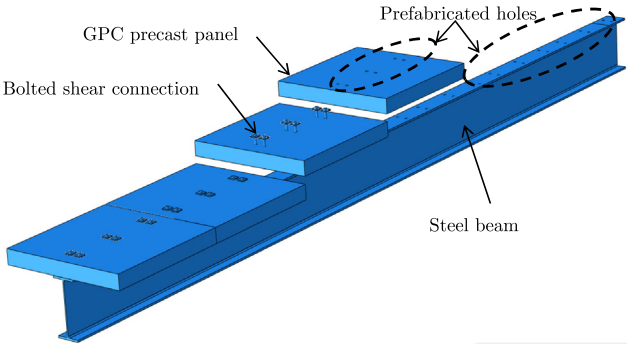

Fig. 1. Schematic outline of sustainable composite beam.

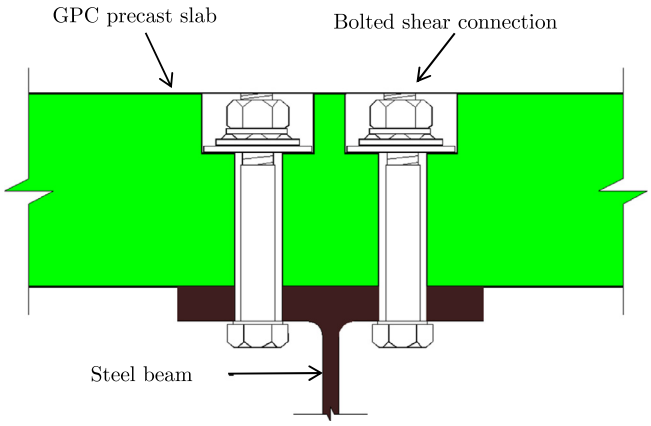

Fig. 2. Cross-sectional configuration of PFBSCs.

the other specimens with PFBSCs. It was considered to be a counterpart to a conventional composite beam, insofar as the concrete was cast *in situ* around the shear connectors. The geometry, dimensions and details of specimen CB1 are illustrated in Fig. 3. The composite action between the concrete slab and steel beam was provided by SEBSCs (Fig. 4a). A total of 56 shear connectors (28 connectors in each shear span) were bolted in pairs on the top steel flange along the beam (Fig. 3) and embedded in the concrete slab. The whole concrete slab was cast with GPC, and Fig. 4b shows a view of this specimen after casting.

Composite beams CB2, CB3 and CB4 were designed with the same configuration, consisting of PFBSCs and precast GPC panels. The difference between them was the number of post-installed bolted shear connectors distributed along the beam.

Specimen CB2 was designed with full shear connection, with the number and spacing of the connectors for specimen CB2 being equivalent to that of specimen CB1; *viz.* a total of 56 post-installed bolted shear connectors of Grade 8.8 M20 bolts (8 bolts per concrete panel) were used in pairs (Fig. 5). In order to confirm the minimum post-tensioning force of 145 kN induced in the M20 bolts, an electric control torque wrench (Fig. 6a) with squirter direct tension indicating washers (Fig. 6b) was used. The concrete slab for specimen CB2 was assembled from seven juxtaposed precast GPC panels installed on the top flange of the steel beam.

Specimen CB3 was designed with 97% shear connection (Fig. 7), having 28 bolted shear connectors (14 connectors in each shear span) and seven precast concrete panels (4 bolts per concrete panel). Beam CB3 is shown in Fig. 8 prior to testing. Specimen CB4 was designed to have 55% shear connection (Fig. 9), having a total of 18 bolted shear connectors (nominally 2 bolts per concrete panel). One additional pair of bolts was used near each end of the

Table 1
Summary of composite beam specimens.

Specimen	Steel beam	Precast concrete slab (mm)	Bolted shear connection type	Total number of bolts	Degree of shear connection
CB1	460	150	Embedded	56	>100
CB2	UB	150	Post-installed	56	>100
CB3	67.1	150	Post-installed	28	97
CB4		150	Post-installed	18	55

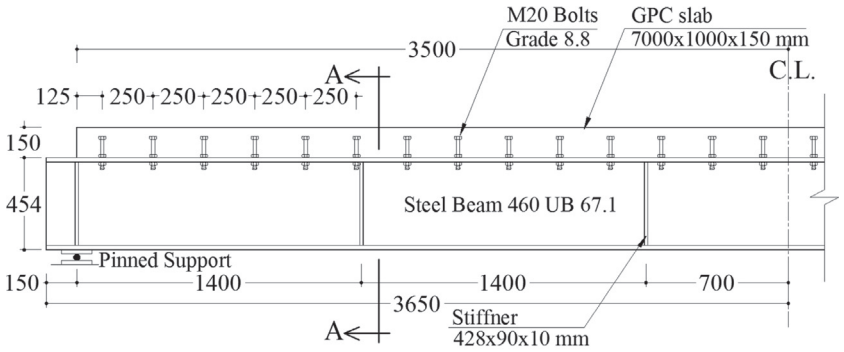

Elevation view

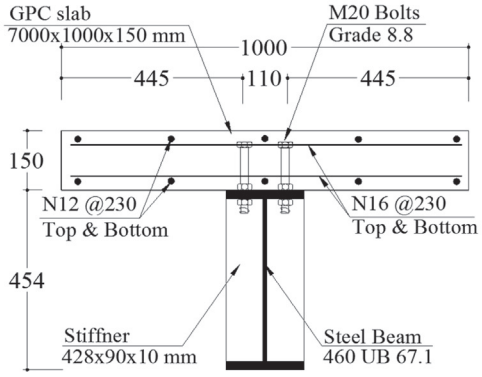

Section A-A

Fig. 3. Geometry and details of composite beam CB1 (unit: mm).

(a) SEBSCs on top flange (b) after concrete casting

Fig. 4. Preparation of specimen CB1.

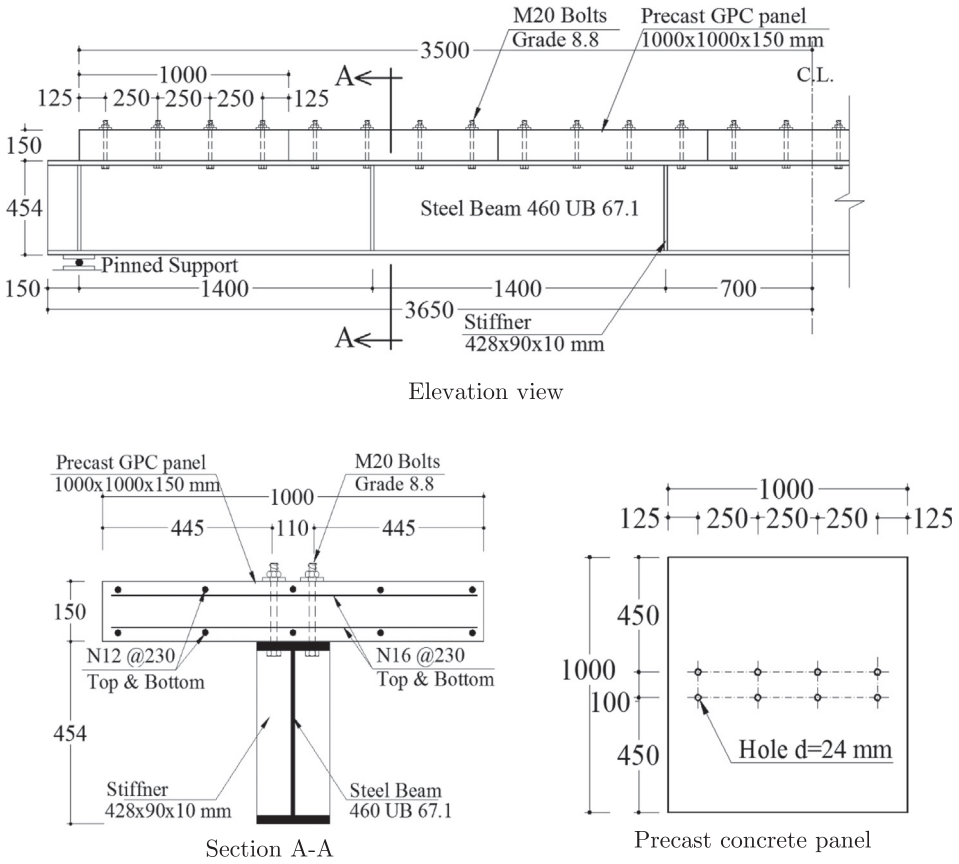

Fig. 5. Geometry and details of composite beam CB2 (unit: mm).

Fig. 6. Tightening of bolted shear connectors.

beam to ensure that a concrete panel would not drop from the beam in the laboratory as a result of bolt fracture.

2.2. Instrumentation

In order to quantify the performance and to elucidate the structural behaviour of the composite beams, linear strain conversion transducers (LSCTs) and strain gauges were mounted on the specimens (Fig. 10). The mid-span and quarter-span vertical displacements of the beams were measured using one LSCT and two laser transducers, respectively. Ten horizontal LSCTs (six along the length of the beam and two at the each end of the beam) were attached to the bottom of the concrete slabs to measure the interface slip between the concrete and the steel beam during the test (Fig. 10). A total of thirty-two strain gauges (sixteen strain gauges with a maximum strain of 10–15% for the steel beam and sixteen strain gauges for the concrete slab) were employed to measure the strains in the steel beam and concrete slab at different locations (Fig. 11).

2.3. Experimental setup and loading procedure

Fig. 12 shows the configuration of the test set-up, with roller and pin supports being located at the ends of specimen to provide simply-supported end conditions. Four displacement-controlled forces were applied on the tested beam using a 5 MN hydraulic jack to simulate a uniformly distributed load. The load was applied to the composite beam through three spreader beams. Prior to the actual test, a small load of about 10% of the predicted ultimate load was applied to the specimen, which was then unloaded, in order to check the test set-up and the performance of the instrumentation. After confirming the functionality of the testing procedure, the

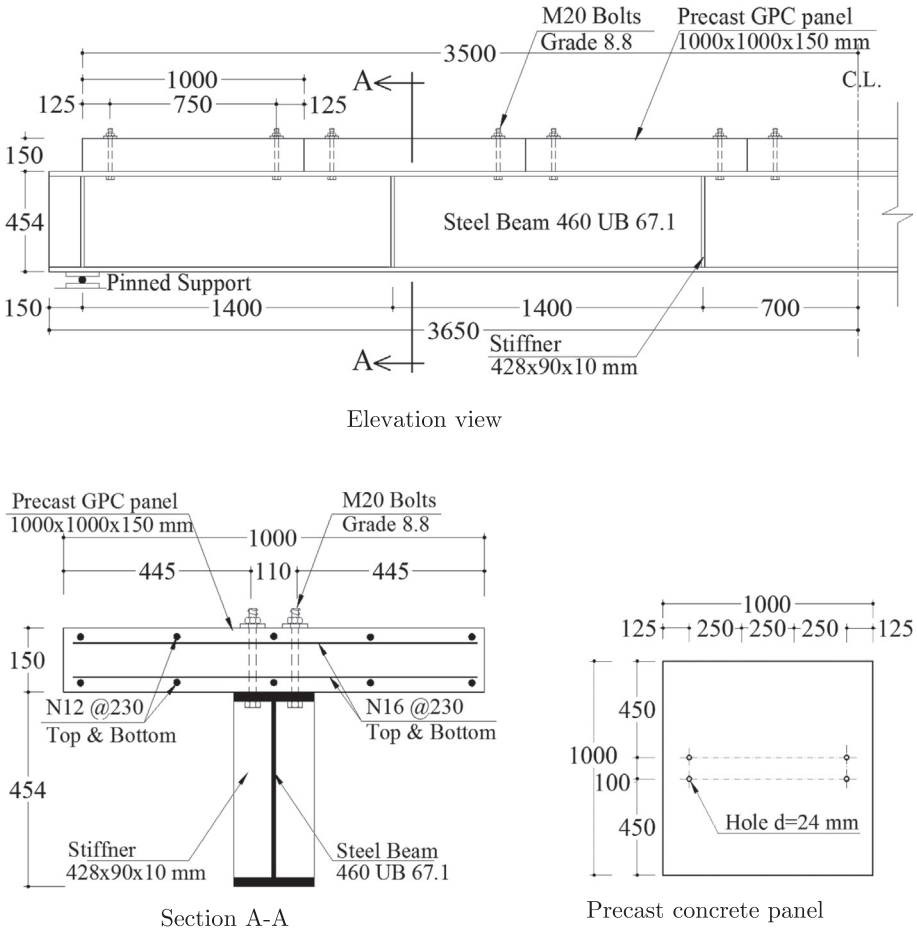

Fig. 7. Geometry and details of composite beam CB3 (unit: mm).

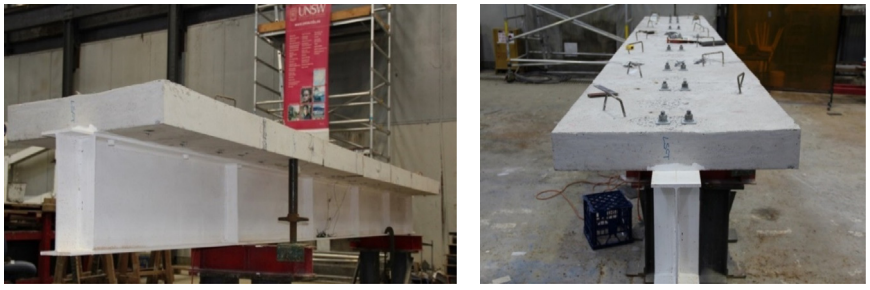

(a) side view showing stiffeners (b) top view showing bolted connectors

Fig. 8. Top view of specimen CB3.

specimens were reloaded under displacement control until no further load could be sustained, and the test was terminated when significant crushing of the concrete slab was evident. Four displacement-controlled loading rates (*i.e.* 0.3 mm/min for the linear range, then 0.6 mm/min, 1.2 mm/min and 2 mm/min for plastic range) were used sequentially. During the test, the top and both side faces of the concrete slab were inspected for the development of cracks, and the top flange of the steel beam for local buckling.

2.4. Material tests

Coupons taken from the flange and web of the steel beams having nominal thicknesses of 12.7 mm and 8.5 mm respectively were tested under tension to determine their modulus of elasticity, yield strength and ultimate tensile strength. The average values of the tensile coupon test results are summarised in Table 2. Direct tension tests were also conducted on the high-strength bolted shear connectors and steel reinforcing bars, and the results are also given in Table 2. GPC with a target compressive cylinder strength at 28 days of 40 MPa was used for the concrete slab. Compressive and indirect tensile tests were conducted on concrete cylinders according to the relevant Australian standards AS1012.9 [17] and AS1012.10 [18], and the results are summarised in Table 3.

Push-out tests were undertaken to characterise the load-slip behaviour of the bolted shear connectors in the composite beams with GPC slabs. The results obtained from the push-out tests were used to determine the degree of shear connection in the design of the composite beams. Four push-out tests (Fig. 13) with M20

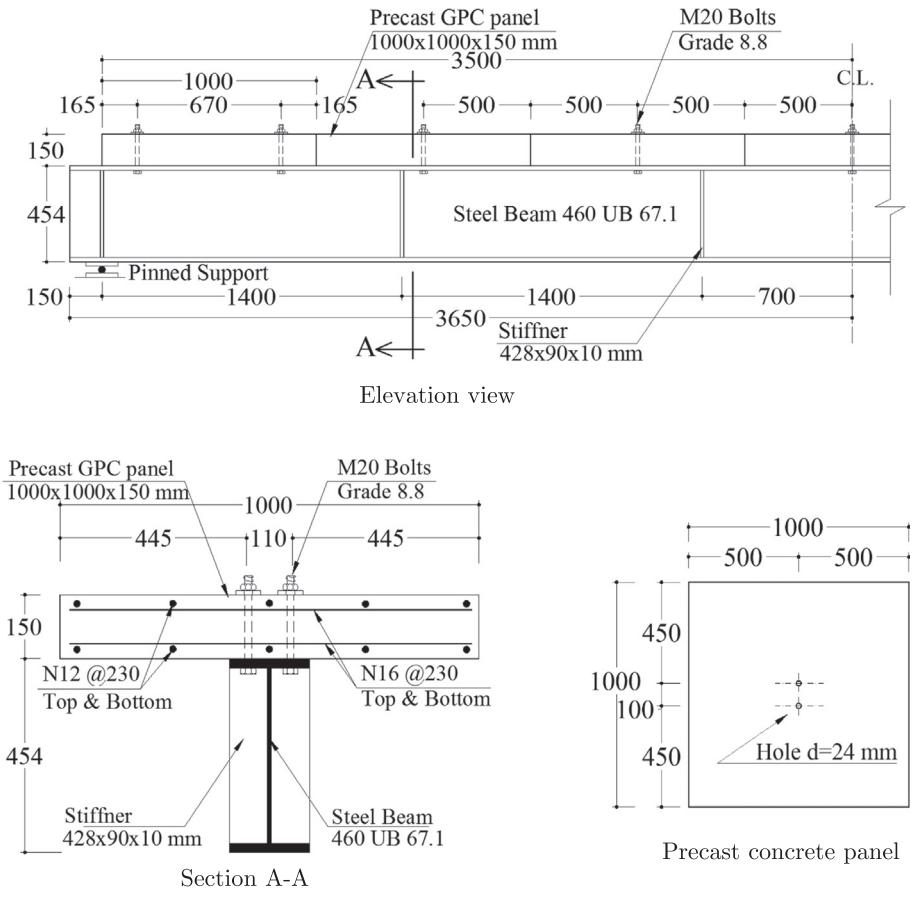

Fig. 9. Geometry and details of composite beam CB4 (unit: mm).

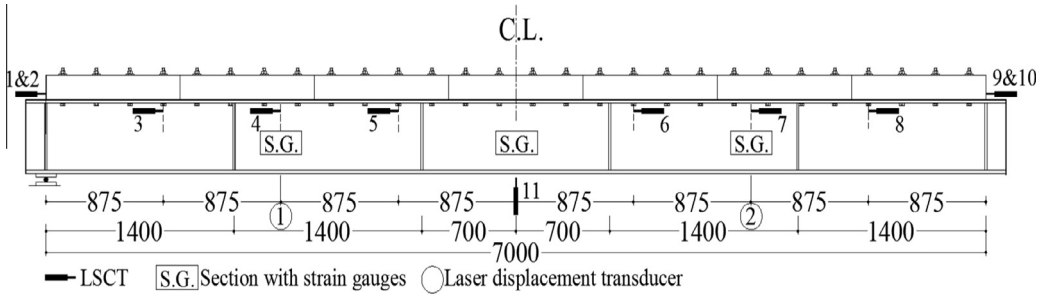

Fig. 10. Layout of beam instrumentation.

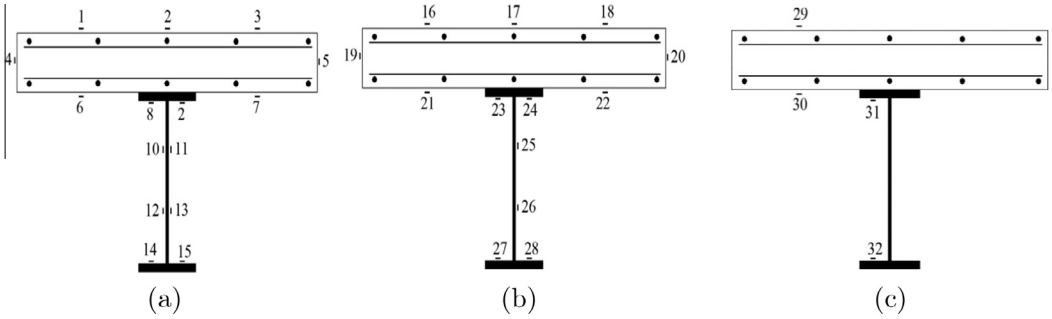

Fig. 11. Strain gauge locations at cross sections of composite beam: (a) mid-span, (b) first quarter span, and (c) third quarter span.

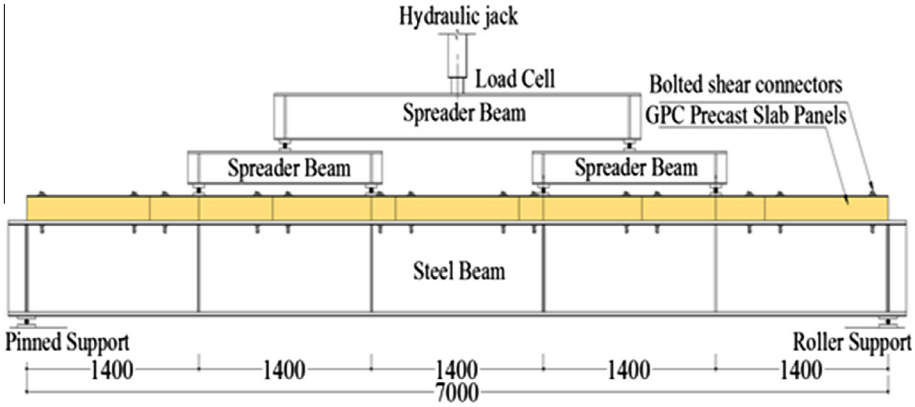

Fig. 12. Configuration of test set-up.

Table 2
Mechanical properties of reinforcing steel bars, steel beams and bolted shear connectors.

Specimen	Yield strength (MPa)	Ultimate strength (MPa)	Young's modulus (GPa)
Steel beam flange	375	496	200
Steel beam web	368	506	205
Bolted shear	936	969	210
Reinforcing bars	543	640	200

Table 3
Compressive and indirect tensile strength of concrete.

Specimen	Compressive strength (MPa)		Tensile (MPa) strength		Young's modulus (GPa)
	28 days	Test day	28 days	Test day	
CB1	44.9	45.8	4.43	4.7	22.1
CB2		43.1		4.8	21.1
CB3		40.9		4.3	21.1
CB4		39.7		4.7	NA

Fig. 13. Push-out test specimens.

bolted shear connectors were designed and conducted in accordance with EC4 [19]. Two push-out tests were performed to examine the load-slip behaviour of PFBSCs in composite beams and the other two on SEBSCs in composite beams. The experimental load versus slip curves are shown in Fig. 14. In designing the beam tests,

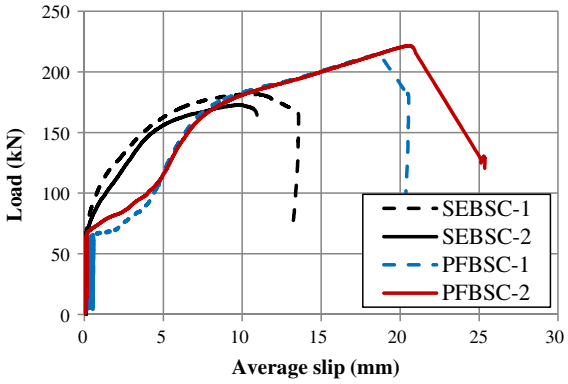

Fig. 14. Load-slip responses of push-out tests.

the degree of shear connection was determined based on the maximum load capacities of the PFBSCs and the SEBSCs obtained in the push-out tests. Details of the push-testing of deconstructable beams have been reported elsewhere [10].

3. Experimental results and discussion

3.1. Crack pattern and failure mode

All composite beams were tested under a monotonically-increasing displacement-controlled quasi-static loading regime and the results are summarised in Table 4.

During the tests, all of the specimens were inspected for the onset of first cracking in the concrete slabs, the local buckling of the steel beam and crushing of the concrete.

The load versus mid-span deflection response of specimen CB1 is shown in Fig. 15. The behaviour of the beam was linear up to 286 kN, followed by a non-linear response resulting from the progression of slip between the concrete slab and steel beam, and then yielding of the steel beam. The points (loads) identified on the equilibrium curve corresponding to first slip between the concrete slab and steel beam at both ends of the composite beam, yielding of the steel beam, the maximum tensile stress in the bottom surface of concrete slab and the maximum compressive stress in the top surface of the concrete slab are shown in Fig. 15. First cracking developed on the soffit of the slab at mid-span at load of 628 kN. As the applied load increased, more vertical cracks observed around the mid-span of the specimen on both sides of the concrete slab (Fig. 16). At a load of about 1000 kN, the cracks were quite visible. The maximum load capacity of 1135 kN was attained at a mid-span

Table 4
Composite beam test results.

Specimen	Initial stiffness, kN/mm	Load		Deflection		Moment		Maximum end slip			Failure mode
		Ult., kN	Final, kN	Ult., mm	Final, mm	Ult., kN m	Final, kN m	West, mm	East, mm	Av., mm	
CB1	31.39	1135	1104	236	236	1191	1159	3.2	3.0	3.1	CC
CB2	23.66	973	887	208	377	1022	932	7.5	5.0	6.3	CC&FB
CB3	21.46	932	855	278	355	979	898	7.8	6.8	7.3	CC&FB
CB4	22.11	909	851	248	367	954	894	9.7	9.8	9.7	CC&FB

Notes: CC = Concrete Crushing; FB = Flange Local Buckling.

deflection of 236 mm for specimen CB1, being 1/30 of the span. The strength of the specimen decreased rapidly beyond 285 mm deflection, due to concrete crushing and the initiation of local buckling of the top flange of the steel beam. The specimen failed due to concrete crushing, accompanied by buckling of the longitudinal bars at the mid-span of composite beam (Fig. 17). It was observed that, in terms of the spalling of the concrete in the compression zone, the response of the GPC was more robust than that of conventional concrete in composite beams.

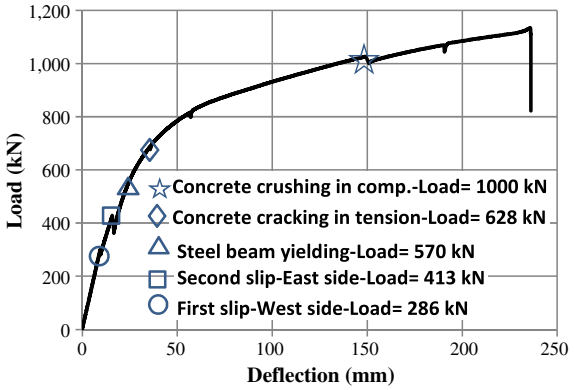

Fig. 15. Load–deflection response of specimen CB1.

Fig. 16. Vertical concrete cracks on bottom and side faces of concrete slab.

Fig. 17. Crushing of concrete slab and local buckling of rebar at mid-span.

The load–deflection response of specimen CB2 measured at the mid-span of the beam is shown in Fig. 18. Similarly to specimen CB1, the behaviour of specimen CB2 was linear up to about 500 kN. As the load was increased, the precast concrete panels located at the ends of the beam started to slip. At a load of about 720 kN, a fine horizontal crack was observed close to the top surface of the concrete panel at mid-span. With the applied load increasing, these horizontal cracks propagated along the concrete slab. The large deflections which developed with increasing loading, in conjunction with the increasing slip, caused different rotations in adjacent panels and this localised the transfer of the compression in the slab, as shown in Fig. 19. The crushing of the top region of the panels in the slab heralded failure of the beam. The ultimate load capacity of specimen CB2 was 973 kN at a deflection of 208 mm, being 1/34 of the span. Following this, the load in the specimen started to decrease with crushing of the concrete and

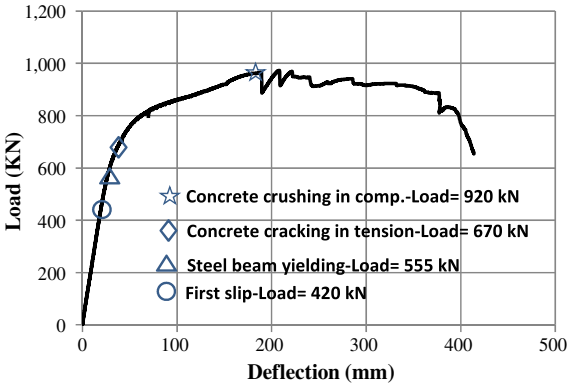

Fig. 18. Load–deflection response of specimen CB2.

Fig. 19. Concrete cracking development of specimen CB2.

the onset of local buckling of the top flange of the steel beam. The final strength of 887 kN at 377 mm deflection was recorded at the end of the test. Fig. 20 shows the beam in the testing rig at the conclusion of the testing.

The behaviour of specimens CB3 and CB4 were generally similar to that of CB2, with the counterpart respective load versus deflection plots being given in Figs. 21 and 22. Like specimen CB2, but unlike CB1 whose slab was monolithic, specimens CB3 and CB4 experienced the development of fine horizontal cracks as the deflections increased and the panels rotated relative to each other. The concentrated reaction at adjacent slabs that results from this creates a situation that is akin to the splitting response in post-tensioned concrete beams. Although specimen CB4 was designed to have 55% shear connection, the failure occurred because of slab crushing and the bolts did not fracture. This is because the push testing procedure, on which the beam design was based, does not allow for relative slab rotations and so does not capture this localised splitting and subsequent crushing effect. Table 4 presents the results for all of the composite beams.

Fig. 20. Specimen CB2 at the conclusion of the testing.

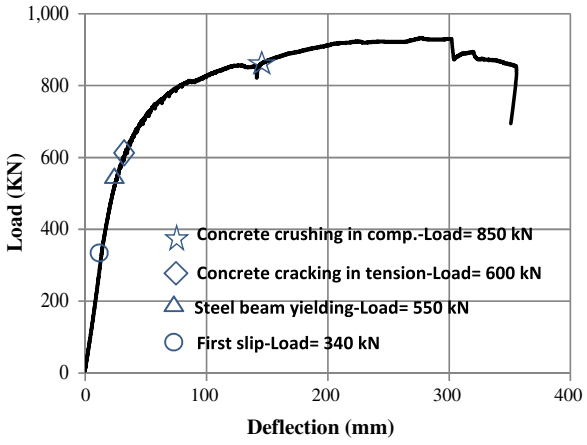

Fig. 21. Load–deflection response of specimen CB3.

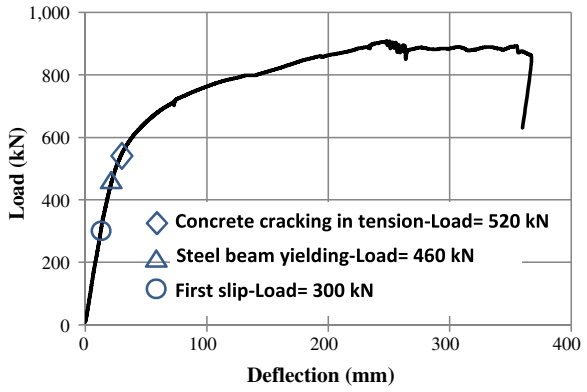

Fig. 22. Load–deflection response of specimen CB4.

3.2. Stiffness, strength and deformation response

Table 4 indicates that the initial stiffnesses of the composite beams were slightly different, due to the differences in the levels of shear connection and the type of the bolted shear connectors. The load versus mid-span deflection curves for all the specimens are compared in Fig. 23. Values of the initial stiffnesses of 31.39 kN/mm, 23.66 kN/mm, 21.46 kN/mm and 22.11 kN/mm were obtained for specimens CB1, CB2, CB3 and CB4 respectively. Specimen CB1 with embedded bolted shear connectors achieved a somewhat higher initial stiffness (32%) than that of specimen CB2. This is because the slab of specimen CB1 used cast in situ GPC which was monolithic, whilst there was some rotation and movement of the panels in the other beam specimens. The initial stiffnesses of all the three composite beams (CB2, CB3 and CB4) with PFBSCs were similar. Specimen CB2 with the highest degree of shear connection achieved 110% and 107% of the initial stiffness of specimens CB3 and CB4, respectively. Nevertheless, it can be concluded that by using tensioned bolted shear connectors, composite beams with partial shear connection can achieve sufficient initial stiffness.

It can be seen from Table 4 and Fig. 23 that specimen CB1 with embedded bolted shear connectors has a higher load capacity (117%) than specimen CB2 with post-installed bolted shear connectors, both being designed to have full shear connection. This is because beam CB1 failed by concrete crushing after the steel had yielded significantly, but beam CB2 was characterised by splitting of the panels that make up the slab due to the concentrated load that is present at adjacent panels when they rotate and slip.

Table 4 and Fig. 23 also show that the specimens with post-installed bolted shear connectors are much more ductile than that with embedded bolted shear connectors, with CB2, CB3 and CB4 having 160%, 150% and 156% of the final deflection of CB1 respectively. The Australian composite structures standard AS2327.1 [16] requires that the mid-span deflection of a composite beam under service load conditions does not exceed 1/250 of the span of the composite beam. It can be seen in Fig. 23 that the load corresponding to this deflection (*viz.* 7000/250 = 28 mm) is around 530 kN for all beams, which corresponds to 47%, 55%, 57% and 58% of the ulti-

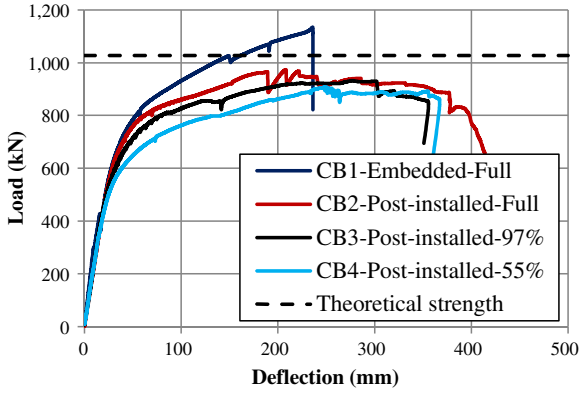

Fig. 23. Load–deflection response of all specimens.

mate loads of CB1 to CB4 respectively. Typically for secondary beams spaced 3 m apart, this corresponds to $530/(7 \times 3) = 25$ kN/m^2, which is many times the service load levels encountered in buildings. It may thus be concluded that all the deconstructable beams considered in this study are very stiff in regard to the serviceability limit state, owing to the frictional resistance at the interface.

3.3. Slips

The maximum slips at the steel–concrete interface for all the specimens obtained from the tests are given in Table 4. It can be seen that specimens CB2, CB3 and CB4 with PFBSCs produced larger end-slips at the end of test than specimen CB1 with SEBSCs. The ultimate end-slip of specimens CB2, CB3 and CB4 were 202%, 237% and 315% of that of specimen CB1 respectively. For the practical installation of the PFBSCs, clearances between the bolt and the pre-fabricated holes in both the steel flange and concrete panels are required. Hence, the composite beams with PFBSCs in clearance holes have a larger slip capacity than the beam constructed using SEBSCs.

The load versus slip response for specimen CB1 is shown in Fig. 24, with first slip occurring at the quarter point at a load of 300 kN first, then at the end at 420 kN. As shown in Fig. 24, three regions of composite behaviour can be identified. Prior to the first slip, the interface friction and bond resist the loading. The second region is categorised by a sudden slip of around 1 mm, which is around the deformation allowed in the clearance holes in the top flange of the steel beam. Following this, the response of beam CB1 is not unlike that of composite beams with headed stud shear connectors welded to the top flange of the steel beam.

Figs. 25–27 show the load-slip curves for specimens CB2 to CB4, whilst Fig. 28 compares the end slips for all beams. It can be seen in Fig. 28 that the responses of the beams with PFBSCs are much more ductile than that with SEBSCs in regard to end slip. Fig. 28 also shows that for the specimen with SEBSCs (*i.e.* CB1) there was a stage where the specimen experienced sudden zero interaction between the concrete slab and steel beam whilst the specimens with PFBSCs (*i.e.* CB2–CB4) did not experience such behaviour during the test. This is most likely because by applying the friction-grip mechanisms, the PFBSCs provide better and more efficient composite action between the precast slab and the steel beam compared with the SEBSCs, which prevent the specimen from developing this sudden zero interaction behaviour.

3.4. Strains and neutral axis

The load versus strain response in the top and bottom flanges of the steel beam at the mid-span and quarter-spans of the composite beams is illustrated in Figs. 29 and 30, respectively. It can be seen that the tensile strains in the bottom flange of the steel beams were much higher than the compressive strains in the top flange. The compressive strains in the top flanges were very small and

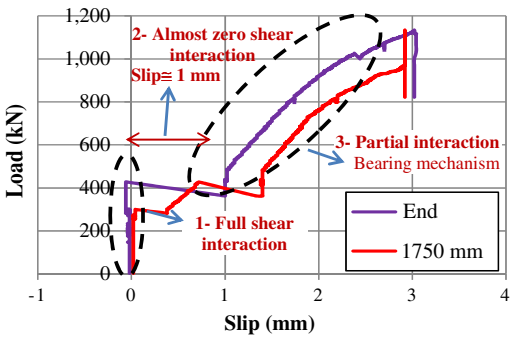

Fig. 24. Load-slip responses of composite beam CB1 with SEBSCs.

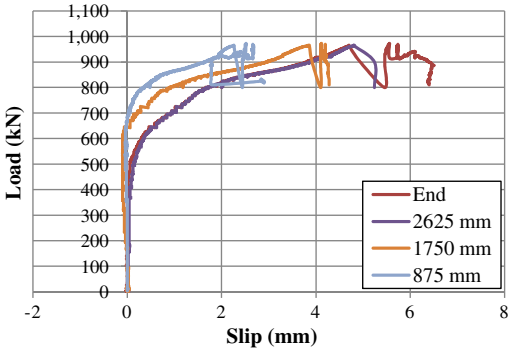

Fig. 25. Load-slip responses of composite beam CB2 with PFBSCs.

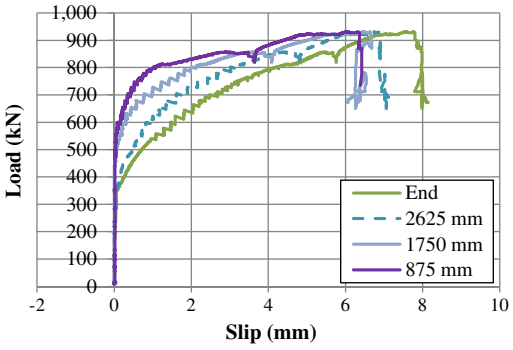

Fig. 26. Load-slip responses of composite beam CB3 with PFBSCs.

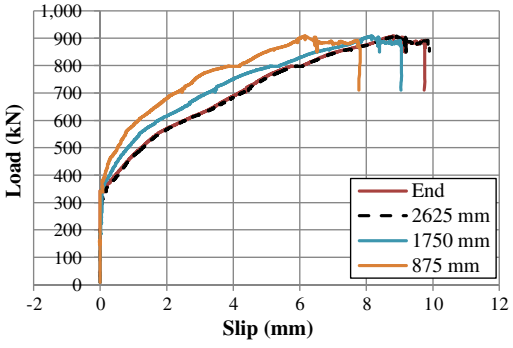

Fig. 27. Load-slip responses of composite beam CB4 with PFBSCs.

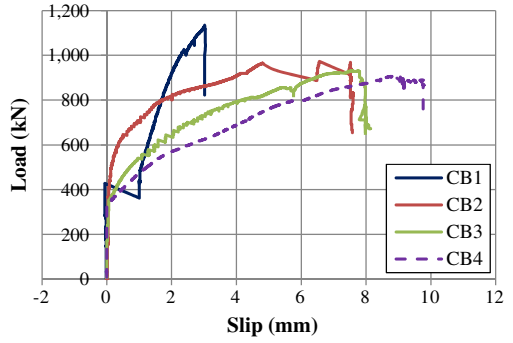

Fig. 28. Load-end slip response of all beams.

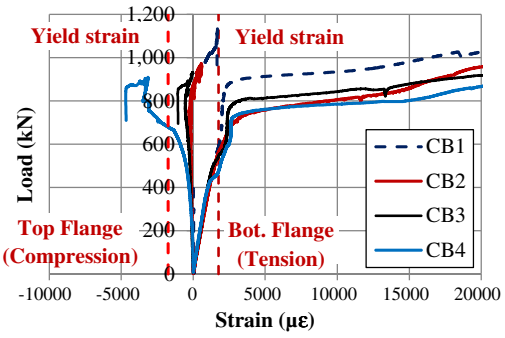

Fig. 29. Load versus strain in bottom and top flange of steel beam at mid-span.

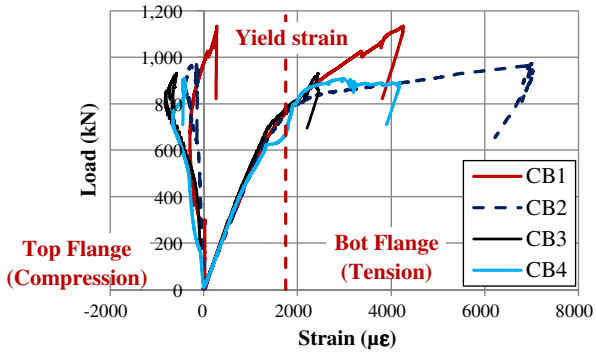

Fig. 30. Load versus strain in bottom and top flange of steel beam at quarter-span.

the neutral axis of the composite beams lay close to the top flange. For specimens CB1 and CB2, as the load increased, the top flange experienced tensile strains as the neutral axis moved into the concrete slab.

The strain distribution through the depth of cross-section at the mid-span is shown in Figs. 31–34 for each of the specimens. The strain distribution for specimen CB1 was almost continuous at the interface of the steel beam and concrete slab, especially at the early stage of loading, with the neutral axes in the steel section and concrete slab being located very close to each other in this specimen. The small discontinuity at the concrete–steel interface was due to the longitudinal slip between the steel beam and concrete slab. It can be concluded that in specimen CB1, almost full composite action was produced by using SEBSCs.

At the early stages of loading, the mid-span strain distribution for specimen CB2 is almost continuous, indicating full shear interaction between the steel beam and precast concrete slab. However, as the load increased, the discontinuity of the strain over the section depth became more prominent indicating a partial shear interaction. Based on the strain distribution, two neutral axes located at the depth of about 420 mm and 505 mm from the base of the section were estimated for the steel beam and the concrete slab, respectively. Specimens CB3 and CB4 have similar strain distributions, with the separation of the two neutral axes increasing with a decrease of the degree of shear connection.

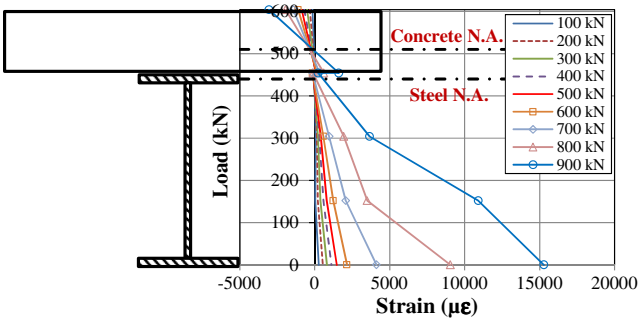

Fig. 31. Strain distributions at mid-span of specimen CB1.

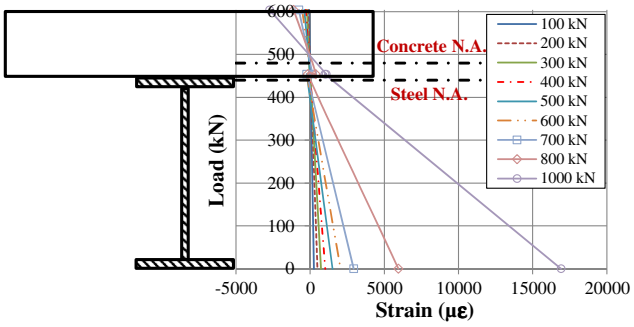

Fig. 32. Strain distributions at mid-span of specimen CB2.

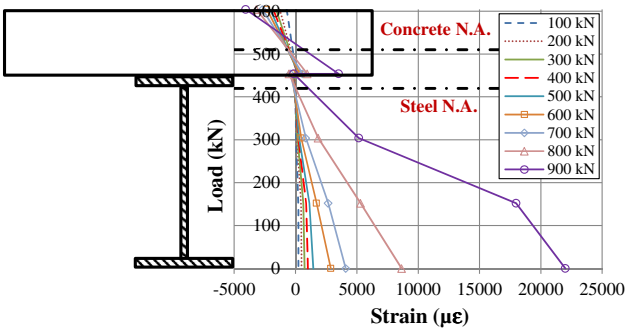

Fig. 33. Strain distributions at mid-span of specimen CB3.

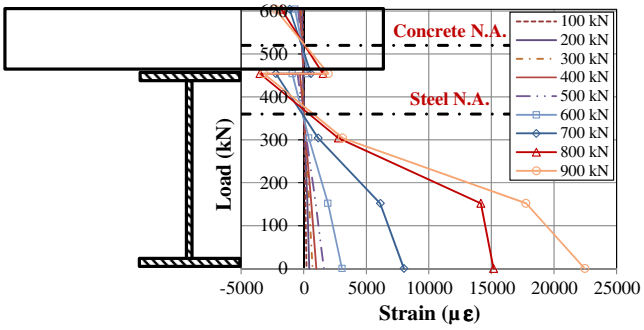

Fig. 34. Strain distributions at mid-span of specimen CB4.

4. Deconstructability

In addition to the structural performance of the composite beams, the deconstructability of the proposed system was also evaluated. To verify that the composite beams can be deconstructed easily at the end of their service life or for other reasons, specimen CB4 was initially loaded to 40% (about 350 kN) of its expected ultimate load, and then cycled 25 times between 5% and 40% of this expected ultimate load (Fig. 35a). Following this, the specimen was then unloaded.

The concrete panel at the western end of the beam was completely removed from the steel section (Fig. 35b) and the beam

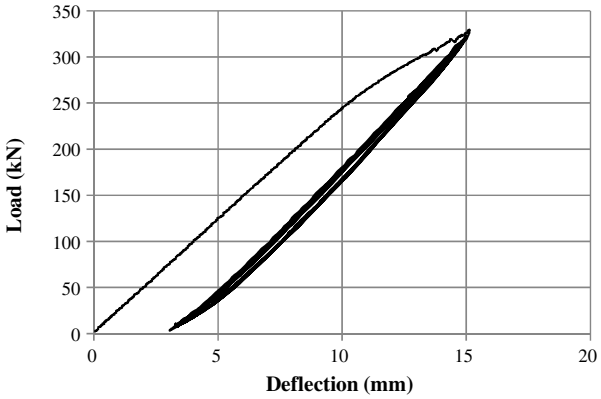

(a) load-deflection response of before dismantling

(b) dismantling

(c) bolted shear connectors after dismantling

Fig. 35. Deconstructability of specimen CB4.

was reassembled with this panel back in place. Subsequently, the specimen was reloaded monotonically until failure as part of the testing program. This procedure demonstrated that composite beams with PFBSCs can be dismantled easily when they have been subjected to loads within the serviceability range, and all components of the system (the steel beam, bolts, nuts and GPC panels) can be reused. The bolted shear connectors after dismantling of the specimen are shown in Fig. 35c.

5. Conclusions

This paper has described tests on composite beams built up from a steel beam, precast geopolymer slab panels with the shear connection being provided by post-tensioned friction-grip bolted shear connectors in clearance holes. Three such beams were tested, as well as one beam with a geopolymer concrete slab cast *in situ* with single-nut embedded shear connectors as a control specimen. The motivation for the tests was to contrive a simple structural system that could be deconstructed and whose components could be reused without wasteful and environmentally-intrusive demolition processes. The response of each beam was assessed under a monotonically increasing quasi-static load under deformation control.

The influences of the type of bolted shear connector, and the degree of shear connection, on the structural performance of this system were investigated, with the details of the experimental findings from these tests being discussed. The results obtained in the experimental work have led to the following conclusions.

1. The use of tensioned friction-grip bolts as shear connectors in composite beams with partial shear connection enables initial stiffnesses close to those with full shear connection to be obtained.
2. Composite beams with single embedded bolted shear connectors with a monolithic slab have a higher ultimate load capacity than counterpart beams with precast concrete panels and post-tensioned friction-grip bolted shear connectors.
3. Composite beams with tensioned friction-grip bolted shear connectors are very ductile when compared with conventional composite beams with headed stud shear connectors.
4. The interface friction between the slab and steel beam induced by tensioning friction-grip bolted shear connectors resists the shear flow force at that location throughout the early stages of loading, allowing for near to full shear interaction.
5. At loads beyond the service load range, the rotation and slip deflections of beams with precast panels localises the transfer of compression in the slab and, as a result, induces longitudinal splitting.
6. Longitudinal splitting and eventual crushing characterises the failure of composite beams having precast panels and tensioned friction-grip bolted shear connectors.
7. Composite beams with precast geopolymer concrete panels for their slabs and attached to the steel beam with tensioned friction-grip bolts in clearance holes can be deconstructed successfully when loaded into the service load range, and the components are able to be reused.

Acknowledgement

The work in this paper was funded by an Australian Laureate Fellowship (FL100100063) awarded to the second author by the Australian Research Council. This support is acknowledged with thanks.

References

[1] Dallam LN. Push out tests with high strength bolt shear connectors. Report for Missouri State Highway Department, Department of Civil Engineering, University of Missouri-Columbia (MI); 1968.
[2] Dallam LN, Harpster JL. Composite beam tests with high-strength bolt shear connectors. Report for Missouri State Highway Department, Department of Civil Engineering, University of Missouri-Columbia (MI); 1968.
[3] Marshall WT, Nelson HM, Banerjee HK. An experimental study of the use of high-strength friction-grip bolts as shear connectors in composite beams. Struct Eng 1971;49:171–8.

[4] Kwon G, Engelhardt MD, Klinger RE. Behavior of post-installed shear connectors under static and fatigue loading. J Construct Steel Res 2010;66:532–41.
[5] Kwon G, Engelhardt MD, Klinger RE. Experimental behavior of bridge beams retrofitted with post-installed shear connectors. J Bridge Eng, ASCE 2011;16:536–45.
[6] Bradford MA, Pi Y-L. Numerical modelling of deconstructable composite beams with bolted shear connectors. In: Conference on numerical modeling strategies for sustainable concrete structures. Aix-en-Provence (France), II-2; 2012. p. 1–8.
[7] Bradford MA, Pi Y-L. Numerical modelling of composite steel-concrete beams for life-cycle deconstructability. In: 1st International conference on performance-based and life-cycle structural engineering. Hong Kong; 2012. p. 102–9.
[8] Bradford MA, Pi Y-L. Nonlinear elastic-plastic analysis of composite members of high-strength steel and geopolymer concrete. Comp Model Eng Sci 2013;2320:1–27.
[9] Pavlovic M, Spremic M, Markovic Z, Budevac D, Veljkovic M. Recent research of shear connection in prefabricated steel-concrete composite beams. J Appl Eng Sci 2014;12:75–80.
[10] Lee SSM, Bradford MA. Sustainable composite beams with deconstructable shear connectors. In: 5th International conference on structural engineering, mechanics and computation. Cape Town (South Africa); 2013.
[11] Ataei A, Bradford MA. FE modelling of sustainable semi-rigid flush end plate composite joints with deconstructable bolted shear connectors. In: International conference on composite construction (CCVII), ASCE, July 2013. Queensland (Australia).
[12] Ataei A, Bradford, MA. Sustainable and deconstructable semi-rigid flush end plate composite joints. In: 1st Australian conference on computational mechanics. Australia, October 2013.
[13] Ataei A, Bradford MA, X. Liu. Sustainable composite beams and joints with deconstructable bolted shear connectors, In: 23th Australian conference on the Mechanics of structures and materials. Byron Bay (Australia), December 2014.
[14] Ataei A, Bradford MA, Liu X. Sustainable and deconstructable flush end plate semi-rigid beam-to-column composite joints. In: 23th Australian conference on the mechanics of structures and materials. Byron Bay (Australia), December 2014.
[15] Ataei A, Bradford MA, Valipour HR. Experimental study of flush end plate beam-to-CFST column composite joints with deconstructable bolted shear connectors. Eng Struct 2015;99:616–30.
[16] Standards Australia. AS 2327.1: Composite structures, part 1: simply supported beams. SA (Sydney); 2003.
[17] Standards Australia. AS 1012 Part 9: determination of the compressive strength of concrete specimens. SA (Sydney); 1999.
[18] Standards Australia. AS 1012 Part 10: method of testing concrete – determination of indirect tensile strength of concrete specimens. SA (Sydney); 2000.
[19] British Standards Institution. Eurocode 4: design of composite steel and concrete structures: Part 1. 1 General rules and rules for buildings, BS EN 1994-1-1. London: BSI; 2006.